Journal of Electroanalytical Chemistry 880 (2021) 114922

Contents lists available at ScienceDirect

Journal of Electroanalytical Chemistry

journal homepage: www.elsevier.com/locate/jelechem

Innovative screen-printed electrodes on cork composite substrates applied to sulfadiazine electrochemical sensing

Ana P.M. Tavares [a,b,c], M. Helena de Sá [b,c], M. Goreti F. Sales [a,b,c,*]

[a] BioMark@UC, Department of Chemical Engineering, Faculty of Science and Technology, Coimbra University, Coimbra, Portugal
[b] BioMark@ISEP, School of Engineering, Polytechnic Institute, Porto, Portugal
[c] CEB, Centre of Biological Engineering, Minho University, Braga, Portugal

ARTICLE INFO

Article history:
Received 4 September 2020
Received in revised form 27 November 2020
Accepted 7 December 2020
Available online 10 December 2020

Keywords:
Cork substrate
Screen-printed electrodes
Carbon electrodes
Molecularly-imprinted polymers
Sulfadiazine

ABSTRACT

This work reports the first use of cork as substrate to produce 3-electrode electrochemical devices, which may be very important to conduct sustainable worldwide biochemical testing in point-of-care. It consists of laminated cork covered by a thin-film of an insulating resin and printed in a 3-electrode system format. Silver ink was used to print electrical tracks and the reference electrode, while carbon ink was used to print working and auxiliary electrodes.
The analytical performance of the cork-based devices was and compared to other common supports, as PET and ceramics in the form of screen-printed electrodes (SPEs). The cork-based devices displayed higher current values and better reversibility features and were able to undergo stable modification with conductive nanomaterials. They were further applied to detect sulfadiazine (SDZ), an antibiotic of human use that is also an environmental contaminant, by modifying the working electrode with a molecularly imprinted polymer (MIP) layer obtained by electropolymerization of pyrrol. The results confirmed the ability of the MIP film to detect SDZ selectively and showed reproducible increasing current signals for increasing concentrations of SDZ, from 8.0 to 186.0 μM. Direct comparison with commercial carbon SPEs showed greater sensitivity for the cork-based SPEs, with 10× lower limits of detection. Overall, cork-based devices are a valuable alternative to currently available SPEs systems, considering environment and cost features and also the analytical gains of this approach. These are especially important in times where a global biochemical testing became necessary for improved public health management.

1. Introduction

Widening point-of-care (POC) analysis is today a worldwide target of Health systems. A medical decision is often supported by the levels of several biomolecules in the blood, saliva or urine, and it would benefit from shifting the conventional laboratorial tests to the doctor's office. POC testing can also be more accurate because it avoids analyte changes during sample transport/storage, caused by delayed release of analytes, by continued metabolism, and by protein/peptide degradation in the whole blood [1,2]. More than ever, in pandemic times, it is clear that a large demand exists for efficient POC devices that provide sensitive and selective readings [3], offering portable and low cost features [4–6].

Mostly considering portability and cost reasons, common POC testing devices such as those of glucose readings make use of screen-printed electrode (SPE) technology. SPEs combine is a small spot working electrode (WE), counter electrode (CE) and reference electrode (RE) [7–9]. Their applications are wide [9] and number of papers published in literature on SPEs and their citations has observed an exponential growth, since 1992 [10]. Moreover, another study forecasts a market over $4.5 billion for fully printed sensors, by 2030 [11].

Screen-printed technology consists of layer-by-layer depositions of ink upon a solid substrate defining the geometry of the intended sensor. In detail, it makes use of a suitable stencil to limit the printing areas and uses a mesh to transfer the ink onto the free substrate surface. A blade is then moved across to fill the open apertures with ink and when the stencil is pulled out the ink remains on the substrate, preserving its printed shape. Subsequent stencil shapes are also possible, allowing overlapping several ink layers with different formats [6,12,13]. Overall, this approach yielded the automated fabrication of commercial SPE devices, containing mostly a three electrode system (WE, CE and RE), printed on a solid substrate of planar format [10,14–16]. This 3-electrode system is ideal for POC analyses, because it allows using small sample volumes, down to the level of few μL. There are however several critical points around SPEs that remain to be improved.

A critical point in assembling SPEs is the ink, usually containing carbon, gold or silver-based conductive materials [17]. Carbon inks consist of

* Corresponding author at: BioMark Sensor Research/UC, Chemical Engineering Department, Faculty of Sciences and Technology, Coimbra University, Rua Sílvio Lima, polo II, 3030-790 Coimbra, Portugal.
E-mail address: goreti.sales@eq.uc.pt. (M.G.F. Sales).

http://dx.doi.org/10.1016/j.jelechem.2020.114922

graphite particles together with other ingredients that are responsible for dispersion and adhesion upon printing [6]. The silver inks are similar to these, but contain a source of silver instead of graphite. In terms of indicating electrodes, the printed surface should be capable of following reproducible modification by different biomolecules, such as protein, antigens, antibodies, enzymes, membrane receptors or nucleic acids. Some conductive inks also have a redox mediator on it, such as metals or metal complexes and pure organic polymers, as Meldola's Blue, Prussian Blue, cobalt phthalocyanine and nickel hexacyanoferrate, etc.. Such inks avoid using an external standard redox probe mediator to monitor the electrical output of the device [7,13,15,18]. However, the exact composition of all these commercial inks is crucial for a suitably printed material. It remains however a secret due to proprietary issues of the commercializing industries.

The substrate where the inks are printed is another critical point. In general, the most common SPEs are printed on plastic, as PET or PVC, and ceramics [6,10,19], or PCB [8]. These supports are expected to display insulating properties, because the electrical path should flow only through the conductive inks printed on top of these substrates. In general, these materials work well on SPEs for POC applications, being the plastic-based ones less robust and cheaper than ceramic-based devices. However, an extended worldwide use of such SPEs with synthetic and non-biodegradable support materials will pose subsequent environmental concerns within time that should be addressed now and "greening" this filed is important [20]. A truly worldwide application of POC devices requires replacing such materials by a naturally-derived compound, provided that this natural compound confers proper electrical and mechanical stability features to the final POC device.

Cork is a natural compound that may act as a good support to produce SPEs for POC applications due to several reasons. It is naturally hydrophobic, has low cost, is readily available and displays good electrical and thermal insulation features, while providing high mechanical robustness. It also allows controlled chemical modification. Cork is composed mainly by polymeric structures and extractives with hydroxyl, aldehyde/ketone and/or carboxylic acid functions [21,22]. After oxidation, these groups may also be easily modified, to ensure suitable binding to other compounds. Moreover, planar cork support may be modified with suitably conductive materials, assembled or casted on top by means of suitable physical or chemical deposition methods.

Thus, this work describes for the first time SPEs assembled on cork composite substrates. The electrochemical behaviour of the cork-based SPEs was evaluated by cyclic voltammetry (CV) against two standard redox probes. To validate the advantages of these cork-based devices, the same inks were casted on PET and ceramic supports and the corresponding SPEs evaluated and compared. This innovative 3-electrode system support was also compared with commercial SPEs having carbon WEs. The carbon WE was further modified with poly(3,4-ethylenedioxythiophene), PEDOT, to assess the feasibility of modifying the electrode area with nanomaterials that are commonly employed in the development of new biosensors [23]. The PEDOT-modified cork-based SPE was also employed to detect Sulfadiazine (SDZ), a sulphonamide antibiotic often detected in the aquatic environment [24–26]. The presence of SDZ or other antibiotics in aquatic media needs urgent monitoring, as it is contributing to antibiotic resistance episodes that threaten the efficiency of currently available antibiotic therapies, thereby endangering global public health. Regarding SDZ in particular, it has electroactive properties, where oxidation of sulpha drugs could occur at the $-NH_2$ group at a positive potential, producing a direct electron transfer of SDZ on the electrode surface [27–29]. Therefore, SDZ is ideal to test the electrocatalytic activity of cork-based SPE towards SDZ oxidation.

To this end, a MIP sensing layer was used to recognized SDZ, due to their low cost and long stability [30,31]. It was assembled in-situ in-situ by electropolymerizing pyrrole in the presence of SDZ, on top a conductive layer of PEDOT. SDZ was then removed from the polymeric layer, to create a sensing film that binds selectively to SDZ. The electrochemical performance of the resulting biomimetic sensor was evaluated by the direct detection of SDZ by differential pulse voltammetry, and this was compared to commercial SPEs prepared similarly.

2. Materials and methods

2.1. Instruments

Electrochemical measurements were made in a potentiostat/galvanostat equipament from Metrohm, Autolab, PGSTAT302N, computer controlled by NOVA 1.11 software. The ceramic (CER) substrates were from old SPEs previously purchased to DropSens; the polyethylene terephthalate (PET) substrates were used as locally purchased; and the cork substrates (CORK) were a composite material provided by Amorim cork industry. These supports were printed with carbon CE, a silver pseudo-RE and a carbon-WE of 4 mm diameter. Commercial carbon SPEs were also tested herein as obtained from Orion® (PET substrate) or from Metrohm, DropSens (CER substrates, DRP-C110). All SPEs were linked to the potentiostat via a switch box from BioTid Electronics.

The morphological and chemical properties of the printed electrodes were analysed by scanning electron microscopy (SEM) and Raman spectroscopy (XRD, Thermo, with confocal microscope). Raman analysis was conducted after focusing the material on the optical microscope with 10× lens, and collecting the spectra with a 3 mW laser 532 nm power, for a 50 slit aperture.

2.2. Reagents and solutions

Along this work, ultrapure Mili-Q laboratory grade (conductivity $^{<}$0.1 μS/cm) was used. Several chemicals with pro-analysis grade were employed throughout. These include potassium hexacyanoferrate III ($K_3[Fe(CN)_6]$) and potassium hexacyanoferrate II ($K_4[Fe(CN)_6]$) trihydrate, obtained from Riedel-deHäen; potassium chloride, obtained from Merck; and hexamine ruthenium (III) chloride, obtained from Acros. The carbon ink used herein was DuPont 7102 and the silver ink was DuPont 5025.

The WE was pre-treated by H_2SO_4 from Sigma Aldrich; 3,4-ethylenedioxythiophene (EDOT) from Alfa Aesar was used to modify the carbon ink in the WE; pyrrol (Py) from Sigma Aldrich was used as functional monomer to produce the sensingpolymer. Britton-Robison (BR) buffer to prepare the solutions involved in the polymerization process and standard SDZ solutions used in calibration process. BR buffer was composed by acetic acid from Analar Normapur, sodium hydroxide from Fluka, phosphoric acid from Riedel-deHäen and boric acid from AppliChem.

Iron probe solutions consisted in the redox pair $[Fe(CN)_6]^{3-/4-}$(negatively charged), with varying concentrations of 1.0, 2.5, 5, 7.5 and 10 mM, in each redox state, and prepared in 0.10 mol/L KCl. Ruthenium probe solutions consisted in the redox pair $[Ru(NH_3)_6]^{2+/3+}$ (positively charged), and were prepared with the same concentrations as the negative probe, also in 0.10 mol/L KCl. A stock standard solution of 5.00 mM SDZ was prepared in BR buffer and the less concentrated SDZ standard solutions were prepared by dilution of the stock standard solution in the same buffer, ranging from 8.0 μM to 186.0 μM.

2.3. Preparation of substrates

Cork substrates (CORK) were laminated materials obtained as provided by Amorim cork industry, with a 0.1 cm thickness, made from cork residues. It was found that it had pores through which the water would diffuse within time, thereby allowing an electrical contact between the electrical paths of the different printed electrodes. This was confirmed by dipping the 3-electrode cork-printed system for 24 h in water (Figs. S1 and S2). To avoid this effect, a water-proof (WP) layer was casted on the laminated cork. This WP layer was obtained by spin coating a solution of a commercial resin, for 60 s, at 1500 rpm. After this, the substrate was dried overnight, at 60 °C.

Substrates used for comparison purposes were CER or PET. CER supports were obtained by cleaning and recovering the ceramic supports of commercial screen-Printed Electrodes (C-SPEs). PET substrates were a transparent thermoplastic polymer, of the polyester family [32]. For

comparison purposes, PET and CER devices-based with a WP layer were also prepared, before ink printing (PET/WP or CER/WP devices).

2.4. Printing the electrodes

Handmade electrodes were printed on the substrate by using a mask that defines the shape of electrodes, their area, and their overall distribution [10,12,14]. The mask used for this purpose is shown in Fig. 1A, as drawn in AutoCAD. This 3D mask was handmade in vinyl material and contained the 3-electrode system (CE, RE and WE). It was placed on top of the substrate and the ink casted there by moving a glass roll through this mask. Several layers of ink were printed to ensure suitable electrical features to the final electrodes. Silver ink was used for printing the electrical paths/connections and the RE. The carbon ink was used for printing WE and CE. The WE and CE had areas of 12.6 mm^2 and 13.5 mm^2, respectively. A picture of the final device is shown in Fig. 1B.

2.5. WE modified with PEDOT

First, the 3-electrode system was cleaned by covering the electrodes with a diluted sulphuric acid solution (0.5 mol/L) and applying five successive cycles from −200 mV to 1500 mV. Next, the PEDOT film was synthetized on top of the WE, by electropolymerizing a 0.01 mol/L EDOT solution, prepared in an electrolyte of 0.1 mol/L KCl. Electropolymerization was achieved by applying a potential of 1.10 V, for 40 s.

2.6. Electrochemical measurements

Electrochemical studies used CV data for about 8-μl probe solution covering the 3-electrode system of the SPE (WE, CE and RE). CV experiments used $[Fe(CN)_6]^{3-/4-}$ or $[Ru(NH_3)_6]^{2+/3+}$ probe solutions, of varying concentrations and prepared in KCl electrolyte. For the $[Fe(CN)_6]^{3-/4-}$ probe, the potential was scanned from −300 mV and + 700 mV, and the concentrations were 1.0, 2.5, 5.0, 7.5 and 10.0 mM. For the $[Ru(NH_3)_6]^{2+/3+}$ probe, the potential was scanned from −500 mV to +100 mV and the concentrations were 1.0, 2.5, 5.0, 7.5 and 10.0 mM. Scanning-rates were varied within 25 mV/s and 500 mV/s, with 30 crossing points (15 successive CV cycles). All measurements were made at ambient temperature.

2.7. Assembling of the sensing element

The MIP for SDZ was assembled on Cork-based electrodes and carbon-SPEs commercially available, by the same approach. First, the carbon WE was electrochemically pre-treated by applying potential from −0.20 V to 1.50 V in 0.50 M H_2SO_4, by cyclic voltammetry (CV), for 5 cycles, with a scan-rate of 0.050 V/s. The SDZ-imprinted film was synthesized on the previously modified carbon surface with PEDOT, by eletropolymerizing

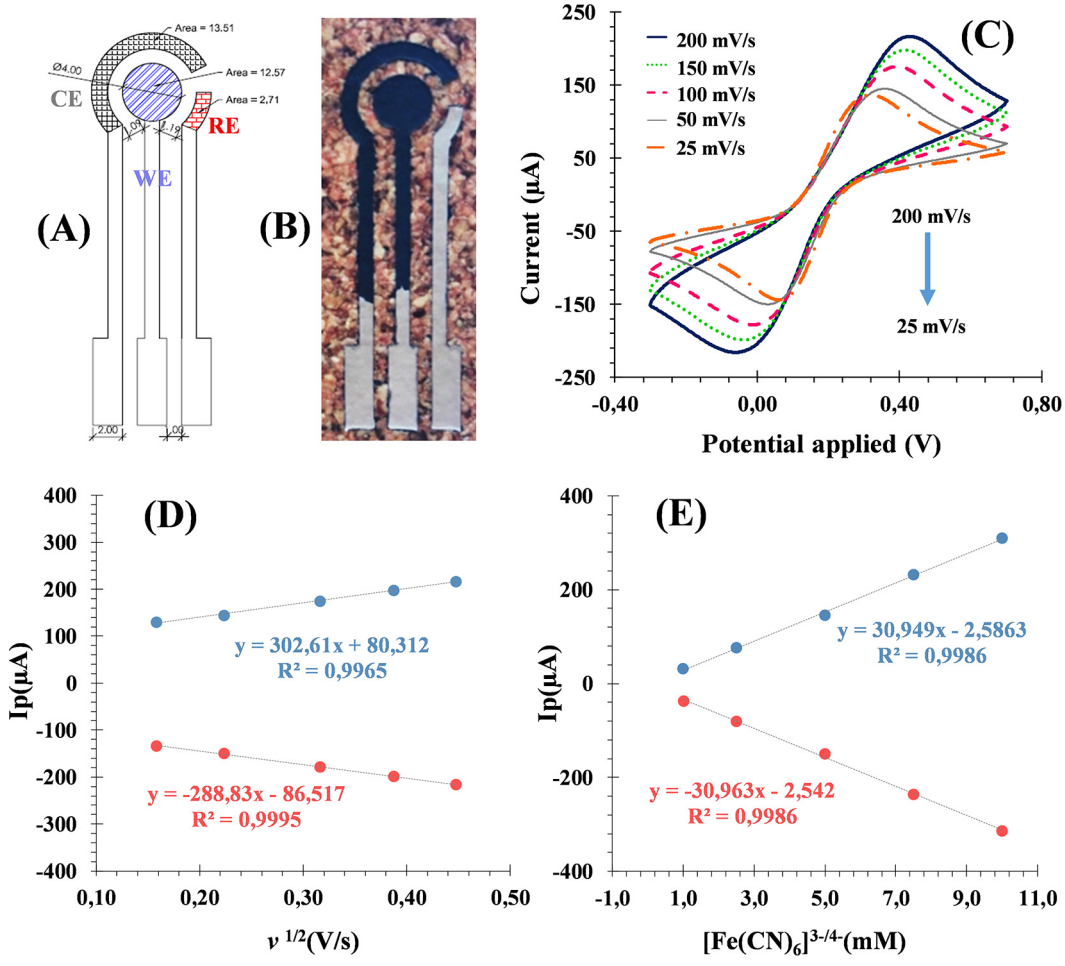

Fig. 1. Schematic representation of the 3-electrode system (A), combining working electrode (WE), counter electrode (CE) and reference electrode (RE); and a picture of the cork-based substrate SPE (B), with conductive paths and RE of silver and WE and CE made of carbon. This goes along with the electrochemical experimental results of the CORK/WP SPE, in terms of (C) Cyclic voltammograms for several scan-rates of a 5.0 mM of redox probe $[Fe(CN)_6]^{3-/4-}$ prepared in 0.10 mol/L of KCl; (D) the plot of the corresponding peak currents against square-root of the scan-rate; (E) and the plot of the anodic and cathodic peak currents for different concentrations of the redox probe $[Fe(CN)_6]^{3-/4-}$, up to 10 mM and prepared in 0.1 mol/L of KCl at 50 mV/s.

2.70 mM Py in the presence of 5.00 mM SDZ, prepared in 40 mM BR buffer, pH 13. The polymeric film was obtained after 10 successive CV cycles, from −0.3 to 0.9 V, with a scan-rate of 0.05 V/s. After this, SDZ was removed by incubating the WE in a solution of 20 mM NaOH. In parallel, a control was produced in the same conditions, using the same approach without antibiotic. The electrochemical performance of the resulting biosensors was evaluated by incubating it in standard solutions of the target compound and monitoring the electrochemical behaviour of the corresponding SPEs after.

3. Results and discussions

3.1. Assembly of cork-based SPEs

The first cork-based electrodes were prepared by direct printing of the inks on the laminated cork. A total of 4-layers of ink were casted in order to produce electrodes with suitable electrical features for electrochemical readings, as demonstrated in [14]. However, with a substantial number of tests on the same Cork-SPE, the electrochemical behaviour started changing, first with electrical drifting and after with an increasing noise, terminating without a measurable signal (Fig. S1). In general, the ink was stably bound to the support, and only the colour of the cork substrate changed, getting darker over time (Fig. S2). This indicated the absorption of water through the cork, which could arise from the intrinsic porosity of cork (Fig. S2C). To check out this possibility, the electrodes were dipped in deionised water for 24 h, without any electrochemical readings (Fig. S2-A). The resulting electrode evidenced water permeation and confirmed the need for a WP layer on the cork, prior to the electrode printing. Eventually, in single use devices this WP layer could be avoided.

Thus, the substrate was modified with a diluted resin casted by spin-coating. As it could impact the electrochemical performance of the Cork-based SPEs, the effect of the WP layer upon the electrochemical response was also tested by preparing cork-based electrodes without (CORK) or with the WP film (CORK/WP), along with the several comparing substrates, also with or without the same WP film.

3.2. Electrochemical features of CORK/WP-based electrodes

The general electrochemical features of the CORK/WP electrodes were first evaluated by checking their behaviour in the presence of 5.0 mM solution of $[Fe(CN_6)]^{3-/4-}$, prepared in KCl electrolyte, and for varying scan-rates (25 to 200 mV/s). To evaluate the electrochemical behaviour and calculate the electroactive area (A) of the WEs, the peak current (I_p) was plotted against the square root of the scan rate [33–36] and its linear trend used. This study followed the *Randles-Sevcik* eq. (S2 in Supplementary Information). The results obtained are shown in table S1, demonstrating that the ratio between the cathodic and anodic peak currents is ~1.0, and that both peak currents increased with scan-rate (Fig. 1C). As expected, a linear trend was observed by plotting the peak current against the squared-root of the scan-rate (Fig. 1D), indicating that the redox reaction of $[Fe(CN)_6]^{3-/4-}$ occurring at the CORK/WP WE/solution interface was controlled by diffusion. The electroactive area of the WE was 9.00 mm^2, representing ~72% of the physical area of the WE.

The electrochemical features of the CORK/WP electrodes were also evaluated (section S2) for increasing concentrations of the same redox probe, 1.0 to 10.00 mM, also prepared in KCl electrolyte, and setting the scan-rate to 50.0 mV/s. The typical results obtained are shown in Fig. 1E, and evidenced increasing anodic and cathodic peak currents with increasing concentrations of the redox couple. The absolute slope value of these linear trends was similar for anodic and cathodic peaks, thereby suggesting that a total charge transfer is occurring at the electrode surface. This also meant that the electrode surface was not being saturated with the redox processes of these electroactive species and that the electron transfer reaction at the electrode surface/solution interface was controlled by diffusion [33,37]. The diffusion coefficient of the redox reaction was 1.73×10^{-5} cm^2/s, which was higher than the theoretical values described in the literature [36,38], therefore indicating that the carbon ink used on the WE surface also acted as electro-catalyst for this reaction [39]. Additionally, the Cork/WP showed reproducible results, obtained with different cork-based electrodes, produced in different days. The anodic peaks resulting from the $[Fe(CN_6)]^{3-/4-}$ probe showed that the signal variations ranged from 0.3 to 5.5% with an average relative standard deviation of 2.6%. The corresponding cathodic peak presented signal variations ranging from 0.6 to 3.4%, with an average relative standard deviation of 1.3%. It is also important to note that the Cork/WP substrates evidenced high chemical stability within at least 5 weeks (time of follow-up), without significant differences, keeping these in a desiccator under an inert atmosphere before use. The chemical composition of the working or reference electrodes on the Cork/WP substrates remained constant over time, considering the low value of relative standard deviation (< 14.5%) of the potential difference between anodic and cathodic peaks (ΔEp).

The behaviour of the CORK/WP substrate in a positively charged redox probe couple was also tested as described in the supplementary information (section S6), confirming a similar behaviour to the iron redox probe.

3.3. Comparison with PET and CER-based electrodes

The electrochemical data of electrodes on PET and CER substrates prepared similarly to CORK/WP substrates are shown in Fig. 2 and discussed in supplementary section S3, Fig. S3. Overall, CORK/WP substrates showed the electrochemical behaviour that was closer to the theoretical reversible redox system, as expected for the $[Fe(CN_6)]^{3-}/[Fe(CN_6)]^{4-}$ redox couple tested (table S1).

The impact of the WP film on the overall electrode performance of PET and CER electrodes was checked by evaluating PET and CER substrates having the same WP film as CORK before ink printing. Compared to CORK/WP devices, PET/WP and CER/WP substrates decreased their ΔE_p for increasing scan-rates. In the case of PET substrates, ΔE_p values varied from 732 to 572 mV without the WP film, and after introducing the WP film the values decreased to 562 and 444 mV (Fig. 2). CER substrates displayed a similar behaviour, with ΔE_p values ranging from 749 to 586 mV without the WP film and decreasing to values ranging from 461.40 to 415.0 mV with the WP film. These results indicated that the WP film improved the kinetics of the redox reaction at the electrode surface, thereby contributing to a faster electron transfer [40]. The ratio between anodic and cathodic peak currents was about the same, but the active area increased in PET/WP and CER/WP-based electrodes, when comparing to the corresponding substrates without the WP layer. The active area obtained for PET/WP and CER/WP were 8.00 mm^2 and 7.00 mm^2, respectively.

Overall, the obtained results indicated that the WP film improved the electrochemical performance of the electrodes prepared in the several substrates, with CORK leading to the best performance. CORK/WP-based electrodes yielded higher peak currents, lower ΔE_p, and higher active area, which indicated that cork was the best material among all substrates evaluated (S1).

3.4. Morphological features of the printed electrode stable

The roughness of WE surfaces prepared in different substrates was examined by SEM imaging of the cross-section of the materials (Fig. 3). The CORK/WP substrate revealed that the carbon layer on the electrode surface (WE) was rougher when compared to that of PET and CER substrates. This could be related to the high porosity of the cork substrate, with lower mass density and higher surface area than the other surfaces, leading to a larger surface area for the same printed ink. In turn, the ink has a carbon layer with some voids throughout the surface, where it may be enhancing the electrochemical behaviour through the surface area available for reaction. Overall, the roughness of the carbon layer surface showed a good agreement with the electrochemical responses of the substrates obtained in the iron redox probe.

A comparison with PET/WP and CER/WP-based electrodes also showed a different surface texture than that of the corresponding substrates without the WP film. The top-view images obtained are shown in Fig. S4 and

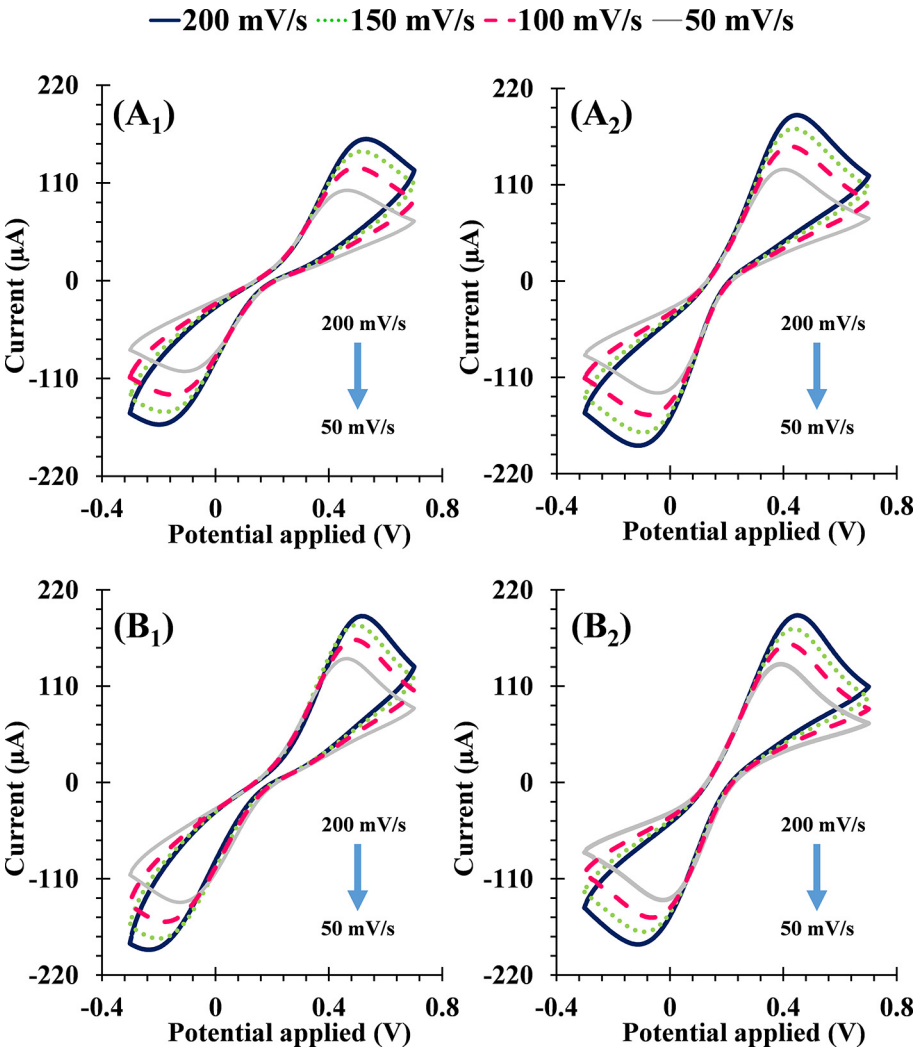

Fig. 2. Cyclic voltammograms of substrates of PET (A) or CER (B) substrates, without (1) or with (2) the WP film having, tested under different scan-rates, for 5.0 mM $[Fe(CN_6)]^{3-/4-}$ solutions prepared in 0.10 M of KCl.

revealed that substrates with the WP layer presented a more heterogeneous surface. Overall, the carbon ink film in the WP-based substrates evidenced a much rougher surface than in substrates without this WP film, thereby inferring a higher electroactive surface area.

3.5. Comparing with commercial carbon SPEs

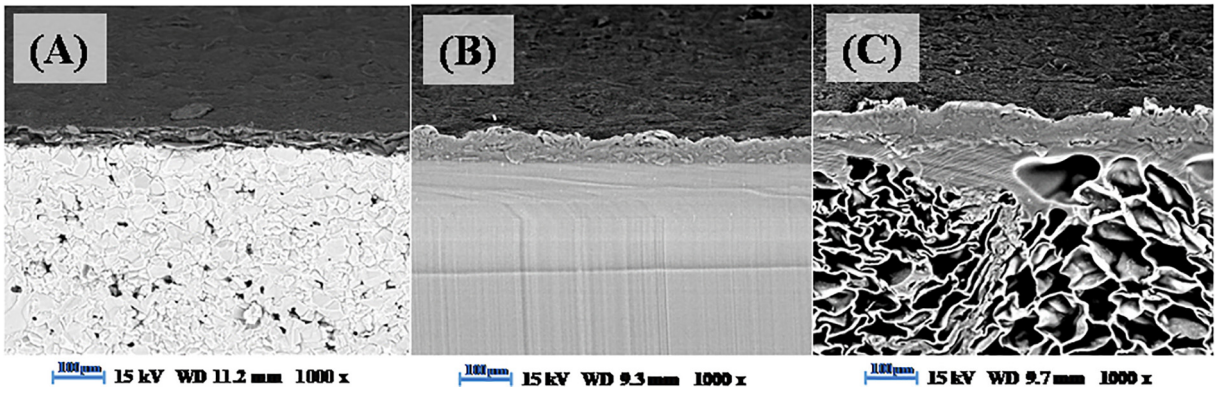

Fig. 3. SEM image of the cross-section of the WE surface in (A) PET, (B) CER, and (C) CORK/WP substrates.

The response of CORK/WP-based electrodes was further compared to that obtained from commercial carbon SPEs based on PET and CER substrates. The results obtained for these commercial versions are shown in

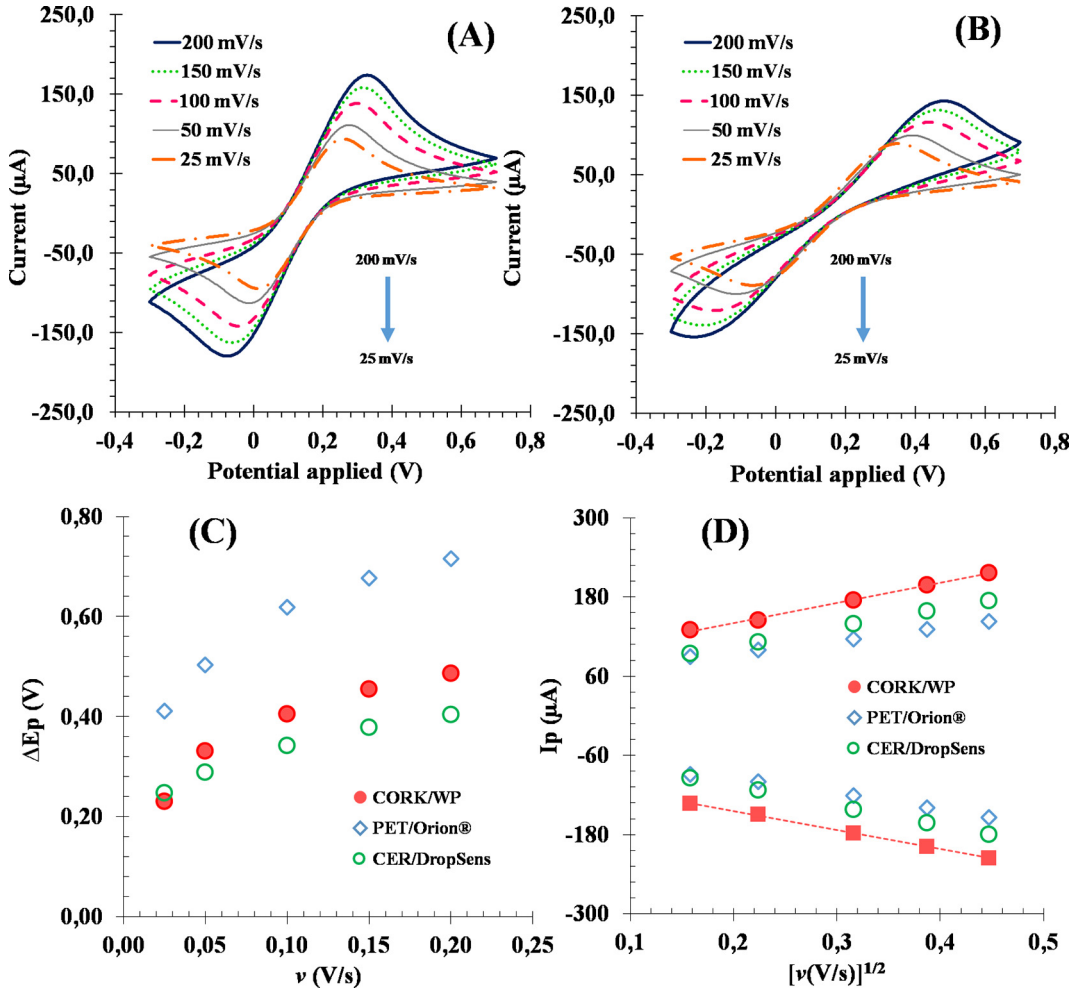

Fig. 4. Cyclic voltammograms for commercial SPEs with 3-electrode systems, printed on (A) CER substrates from *Metrohm Dropsens* and (B) PET substrates from Orion®, evaluated in a 5.0 mM solution of $[Fe(CN_6)]^{3-/4-}$, prepared in 0.10 mM KCl, and evaluated under different scan-rates.

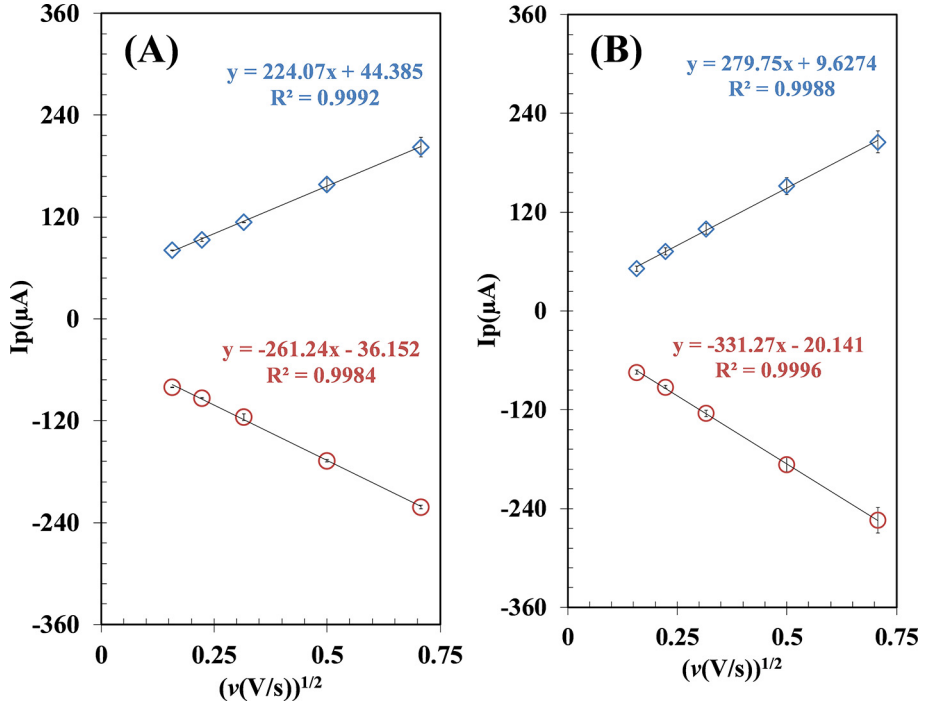

Fig. 5. Plot of the Carbon ink surface between the anodic and cathodic peak currents and squared-root of the scan-rate for (A) $[Fe(CN_6)]^{3-/4-}$ and (B) $[Ru(NH_3)_6]^{2+/3+}$.

Fig. 4 and explained in section S5, Fig. S5, confirming that the CORK/WP electrodes displayed better performance. It is highlighted herein that the electroactive area of the CORK/WP devices (9.0 mm^2) remains the highest among all electrodes tested (5.0 or 8.0 mm^2 for PET or CER substrates, respectively), justifying their higher current values during the electrochemical processes.

Globally, the CORK/WP-based SPEs showed the best electrochemical behaviour, yielding the higher current values and the best reversibility features of the reversible redox couple $[Fe(CN_6)]^{3-/4-}$, among all designs tested. This behaviour was consistent when a positively charged redox probe couple was tested (Fig. 5), as described and discussed in the section S6. Overall, this behaviour anticipates a higher sensitivity for (bio)sensing devices prepared with the innovative CORK/WP substrates described herein.

3.6. Application to sulfadiazine detection

3.6.1. Modification with PEDOT

The use of an SPE as a biosensor requires chemical modifications with sui nanomaterials [6], tested herein by adding a PEDOT layer to the WE, a common modification among biosensors [41,42]. It was made by electropolymerizing EDOT in-situ, a most convenient approach for employing a little amount of solution and taking few seconds to implement. Table.

The electrochemical performance of the PEDOT modified CORK/WP WE was evaluated as in previous studies. The most prominent feature out coming from the presence of PEDOT was the great increase in peak currents (Fig. S7), which directly contributed to the greater sensitivity of the currents measured, and the narrower difference between the peak potentials of the oxidation and reduction peaks. The average data is listed in S2. The plot between peak current (anodic and cathodic) and the squared-root of the scan-rate showed a linear trend for both redox species (Fig. 6), which meant that the electrochemical interaction with PEDOT was also controlled by diffusion. The sensitivity of the current changes in the WE with PEDOTtable was higher than that using only the printed carbon electrodes, increasing by 2.7× for $[Fe(CN_6)]^{3-/4-}$ and 1.6× for $[Ru(NH_3)_6]^{2+/3+}$, as estimated by the Randles-Sevcik equation. The introduction of this PEDOT layer also had an impact on the ΔE_p values (Fig. S8) and the electroactive area of the WE of the cork-based devices. Considering CV studies with the $[Ru(NH_3)_6]^{2+/3+}$-based probe, the active area increased from 7.6 to 12.5 mm^2, and with the $[Fe(CN_6)]^{3-/4-}$ probe the active area increased from 9.0 to 16.8 mm^2 (table S2). Overall, it was clear that the active area increased with this PEDOT coverage, regardless the redox probe used, but this increase was more significant when the iron-based probe was employed.

The profile of the Raman spectra confirmed the presence of PEDOT on the surface of the electrode, showing the typical shape Raman spectra of PEDOT. Compared with the printed carbon WE, there were two peaks in the PEDOT film that are highlighted, located at 1436 cm^{-1} and 1511 cm^{-1} Raman shift (Fig. S9).

Overall, the previous data confirmed the successful modification of the WE of the CORK/WP, yielding homogeneous coverage of the surface. The approach taken herein was also leading to significant improvements in terms of electrochemical performance of the CORK/WP electrodes.

3.6.2. Assembly of MIP on CORK/WP-PEDOT

The CORK/WP-PEDOT was further modified with a MIP material for SDZ, aiming to confirm the utility of the new CORK/WP SPEs for analytical purposes. According to literature, SDZ can be detected directly by electrochemical tools, following the oxidation of the $–NH_2$ group and reduction of the $–SO_2NH–$ group [27]. Herein, SDZ was monitored through the oxidation of the $–NH_2$ group, using DPV to follow this oxidation peak [27–29]. The reduction of $–SO_2NH–$was at − 0.7 V and could suffer from the interfering effect of atmospheric components.

The MIP film was assembled on top of the CORK/WP-PEDOT electrode by electropolymerizing Py in the presence of SDZ. Yet, specific conditions needed to be found in which Py oxidized and SDZ did not undergo oxidation, to allow imprinting the correct SDZ structure (Figs. S10 and S11).

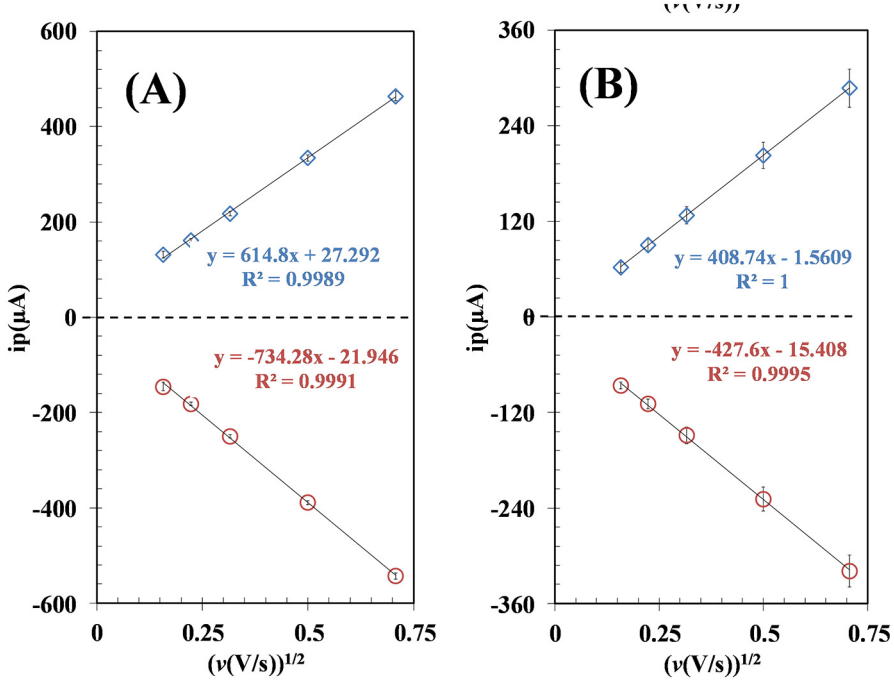

(D)

Fig. 6. Plot of the PEDOT surface between (A) the anodic and cathodic peak current for $[Fe(CN_6)]^{3-/4-}$ against the squared root of the scan-rate; (B) the anodic and cathodic peak currents for $[Ru(NH_3)_6]^{2+/3+}$ against squared root of the scan-rate.

To this end, the electrochemical behaviour of SDZ and Py (single solutions) was studied in BR buffer (40 mM), for pHs ranging from 8.00 to 13.00, by CV scanning between − 0.30 V and + 1.50 V, at a scan-rate of 0.05 V/s. In general, increasing pHs reduced the electroactivity of SDZ but increased the electro-oxidation of Py by decreasing its peak potential (Fig. S12). Thus, pH 13 was used for assemble the MIP film. The extraction of SDZ from the poly(Py) film was made after by incubating the MIP in aqueous alkaline solution. DPV was used to follow this extraction (Fig. 7E). In general, an oxidation peak at + 0.67 V was evident after electropolymerization, which disappeared after extracting SDZ from the polymer. A control material, which was a non-imprinted polymeric (NIP) film, confirmed this by showing no peak. This NIP material was prepared in the same way as the MIP but without SDZ, thereby serving as control of the non-specific binding.

3.6.3. Analytical features

The electrochemical performance of CORK/WP-PEDOT-MIP was evaluated by consecutive incubation of SDZ standard solutions of increasing concentrations, and monitoring after each incubation the amount of SDZ bound. This was done by DPV carried out under the optimal experimental conditions (potential range from 0 V to + 0.9 V, at scan rate 10 mV/s, pulse amplitude 10 mV and pulse width 50 ms with a pre-accumulation potential of − 0.30 V, for 360 s), in 40 mM BR buffer, pH 10 (as described in section S9). In general, increasing concentrations of SDZ yielded increasing peak currents, displaying a linear behaviour against SDZ concentration (Fig. 8) with a slope of 0.0022 μA/μM. Calibrations of the control material confirmed the selective and sensitive SDZ binding features of the MIP, because the NIP displayed a slope of 0.0016 μA/μM, with highly irreproducible data, accounting relative standard deviations up to 74%.

For comparison purposes, the same MIP film was assembled on top of commercially available carbon CER-based SPEs with the same PEDOT film on top. The results obtained confirmed the higher sensitivity (0.0022 μA/μM) of the CORK/WP-based electrodes (Fig. 8D), against 0.0014 μA/μM from commercially electrode. Moreover, as one can be in Table 1, CORK/WP-based electrodes presented a wider linearity range for SDZ concentration, with lower limit of detection (LOD) and limit of quantification (LOQ), in comparison with the electrodes made with the commercial SPE. LOD and LOQ values were calculated as the concentration corresponding to, respectively, three and ten times the standard deviation of the blank measurements (in the absence of template molecule). Globally, calibrations of CORK/WP-PEDOT-MIP showed a higher sensitivity (by ~60%) and better LOD (4.22 μM) in comparison with CER-PEDOT-MIP (12.76 μM). The LOQ values of the electrode with CORK/WP or CER based substrates were 6.04 or 13.67 μM, respectively, thereby confirming the better analytical performance promoted by the cork material.

Overall, this data confirmed that using SPEs with higher blank current signals amplified the electrical response, yielding more sensitive calibrations with lower LODs and favouring the accuracy and precision of the analytical method. Moreover, these results opened the possibility of using CORK/WP substrates in an easy way to produce carbon-SPEs that are more sensitive than the ones currently available in the market, yielding homogeneous coverage surfaces upon their modification. Environmental advantages are also anticipated by this approach.

4. Conclusions

Cork was found herein an advantageous alternative substrate for the preparation of electrochemical 3-electrode systems for (bio)sensors, incorporating electrically conductive layers by means of the typical screen-printing techniques. Although it required a water-insulating thin film (WP) to avoid water penetration though its pores, an exhaustive comparison against other substrates confirmed that the inherent properties of cork are behind the best electrochemical features observed (sensitivity, reversibility and reproducibility). This comparison included testing against concurring substrates of PET and CER, prepared by the same screen-printed approach and materials, with or without this WP film, and it was clear that great electrical benefits arise from the presence of cork. Further comparison to commercially available SPEs also confirmed the benefits of using cork. In addition, when CORK/WP substrates were modified with poly(EDOT), it was clear that a uniform layer of polymeric film was formed in-situ, thereby confirming its suitability for subsequent modification. The possibility of using the new cork-devices for analytical purposes was successfully explored by modifying the WE with a suitable MIP film assembled in-situ, which was more sensitive to SDZ than analogous commercial devices.

Overall, cork-based SPEs displayed excellent electrochemical features when compared to other 3-electrode systems. Moreover, cork offers the advantage of being a natural, renewable and low-cost material, which further contributes to reduce the environmental impact from disposed of SPEs after biochemical testing. This is a very important aspect, especially in Health, that may open doors towards the worldwide sustainability of (bio)medical point-of-care devices.

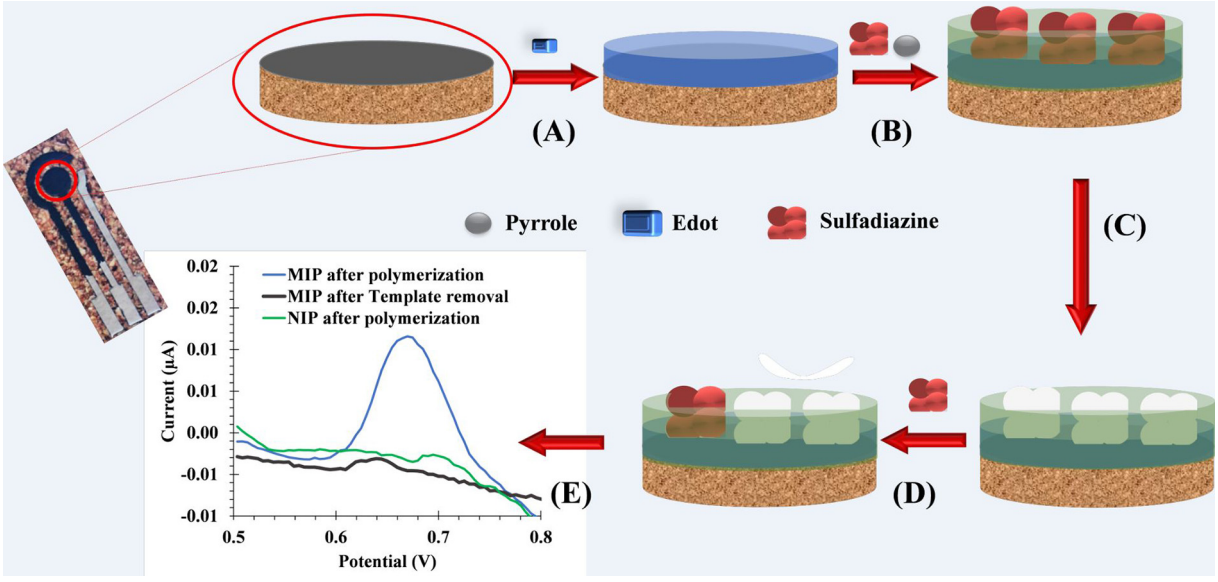

Fig. 7. Synthesis of biomimetic sensor for detection Sulfadiazine. (A) Electropolymerizing EDOT; (B) Electropolymerizing Py in presence of template; (C) Template removal; (D) Rebinding the molecule to the biomimetic sensor; and (E) DPV signal generated by the sensor in the molecule recognition process.

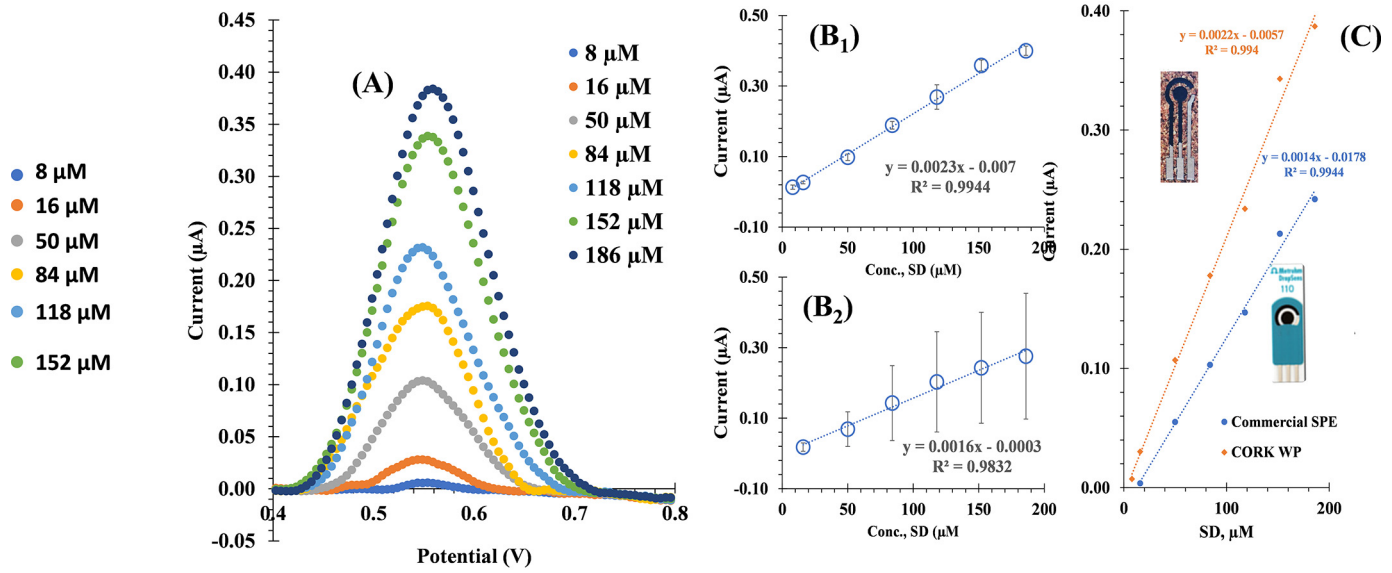

Fig. 8. DPV voltammograms of (A) CORK/WP electrodes in SDZ solutions of different concentrations from 8 µM to 186 µM, prepared in 0.04 M Britton-Robison buffer, at 10 pH, and (B) the calibration curves obtained for CORK/WP-PEDOT-MIP (B_1) and CORK/WP-PEDOT-NIP (B_2), with the application of an accumulation potential of −0.3 V, for 360 s. In (C), the typical calibration of CORK/WP (orange line) electrodes compared to that of commercial electrodes (blue line).

Table 1
Comparison of the different sensors for sulfadiazine detection, using different substrates electrodes.

Substrate	LOD	LOQ	Sensitivity	Linearity range
CORK/WP	4.22 µM	6.04 µM	0.0022 µA/µM	8 µM - 186 µM
Commercial SPE	12.76 µM	13.67 µM	0.0014 µA/µM	16 µM - 186 µM

Declaration of Competing Interest

The authors declare that they have no known competing financial interests or personal relationships that could have appeared to influence the work reported in this paper.

Acknowledgements

This work was supported by Fundação para Ciência e a Tecnologia, I.P. and FEDER (European Funding or Regional Development), via COMPETE2020-POCI (operational program for internationalization and competitiveness), through the project PTDC/AAG-TEC/5400/2014, POCI-01-0145-FEDER-016637. CeNTI – Centro de Nanotecnologia e Materiais Técnicos, Funcionais e Inteligentes is acknowledged for an initial involving the automated screen-printing and Amorim Cork industries for providing the laminated cork.

Appendix A. Supplementary data

Supplementary data to this article can be found online at https://doi.org/10.1016/j.jelechem.2020.114922.

References

[1] E. Schleicher, The clinical chemistry laboratory: current status, problems and diagnostic prospects, Anal. Bioanal. Chem. 384 (1) (2006) 124–131.
[2] C.D.C. Chin, Sau Yin, Tassaneewan Laksanasopin, Samuel K. Sia, Low-Cost microdevices for point-of-care testing, in: W. Issadore, R.M. D (Eds.), Point-of-Care Diagnostics on a Chip, Springer, Verlag Berlin Heidelberg, 2013.
[3] K. Baryeh, S. Takalkar, M. Lund, G. Liu, 1 - Introduction to medical biosensors for point of care applications, in: R.J. Narayan (Ed.), Medical Biosensors for Point of Care (POC) Applications, Woodh Publ 2017, pp. 3–25.
[4] J. Wang, Electrochemical biosensors: towards point-of-care cancer diagnostics, Biosens. Bioelectron. 21 (10) (2006) 1887–1892.
[5] S.K. Vashist, P.B. Luppa, L.Y. Yeo, A. Ozcan, J.H.T. Luong, Emerging Technologies for Next-Generation Point-of-Care Testing, Trends Biotechnol. 33 (11) (2015) 692–705.
[6] H.M. Mohamed, Screen-printed disposable electrodes: pharmaceutical applications and recent developments, TrAC-Trend Anal Chem 82 (2016) 1–11.
[7] A. Hayat, J.L. Marty, Disposable screen printed electrochemical sensors: tools for environmental monitoring, Sensors 14 (6) (2014) 10432–10453.
[8] F.T.C. Moreira, M.J.M.S. Ferreira, J.R.T. Puga, M.G.F. Sales, Screen-printed electrode produced by printed-circuit board technology. Application to cancer biomarker detection by means of plastic antibody as sensing material, Sensor Actuat B-Chem 223 (2016) 927–935.
[9] K. Yamanaka, M.D.C. Vestergaard, E. Tamiya, Printable electrochemical biosensors: a focus on screen-printed electrodes and their application, Sensors (Basel, Switzerland) 16 (10) (2016) 1761.
[10] M.U. Ahmed, M.M. Hossain, M. Safavieh, Y.L. Wong, I.A. Rahman, M. Zourob, E. Tamiya, Toward the development of smart and low cost point-of-care biosensors based on screen printed electrodes, Crit. Rev. Biotechnol. 36 (3) (2016) 495–505.
[11] G. Chansin, Printed and Flexible Sensors 2015–2025: Technologies, Players, Forecasts Established and emerging markets - the complete picture on all applications: biosensors, temperature, humidity, gas, capacitive, piezoresistive, piezoelectric, photodetectors, 2015 https://www.idtechex.com/en/research-report/printed-and-flexible-sensors-2015-2025-technologies-players-forecasts/428 (Accessed March, 03 2020).
[12] Z. Taleat, A. Khoshroo, M. Mazloum-Ardakani, Screen-printed electrodes for biosensing: a review (2008-2013), Microchim. Acta 181 (9–10) (2014) 865–891.
[13] M. Li, Y.T. Li, D.W. Li, Y.T. Long, Recent developments and applications of screen-printed electrodes in environmental assays-a review, Anal. Chim. Acta 734 (2012) 31–44.
[14] M.C.C.G. Carneiro, F.T.C. Moreira, R.A.F. Dutra, R. Fernandes, M.G.F. Sales, Homemade 3-carbon electrode system for electrochemical sensing: application to microRNA detection, Microchem. J. 138 (2018) 35–44.
[15] F.T.C. Moreira, B.A.G. Rodriguez, R.A.F. Dutra, M.G.F. Sales, Redox probe-free readings of a beta-amyloid-42 plastic antibody sensory material assembled on copper@carbon nanotubes, Sensor Actuat B-Chem 264 (2018) 1–9.
[16] G.V. Martins, A.C. Marques, E. Fortunato, M.G.F. Sales, Wax-printed paper-based device for direct electrochemical detection of 3-nitrotyrosine, Electrochim. Acta 284 (2018) 60–68.

[17] S. Cinti, D. Neagu, M. Carbone, I. Cacciotti, D. Moscone, F. Arduini, Novel carbon black-cobalt phthalocyanine nanocomposite as sensing platform to detect organophosphorus pollutants at screen-printed electrode, Electrochim. Acta 188 (2016) 574–581.
[18] Dropsens, Screen-Printed Electrodes, 2016 , (Accessed April, 25 2016) http://www.dropsens.com/en/screen_printed_electrodes_pag.html.
[19] G. Ozcelikay, L. Karadurmus, S.I. Kaya, N.K. Bakirhan, S.A. Ozkan, A review: new trends in electrode systems for sensitive drug and biomolecule analysis, Cr Rev Anal Chem 50 (2020) 212–225.
[20] P.K. Kalambate, Z. Rao, J. Wu Dhanjai, Y. Shen, R. Boddula, Y. Huang, Electrochemical (bio) sensors go green, Biosens. Bioelectron. 163 (2020) 112270.
[21] I.M. Aroso, A.R. Araújo, R.A. Pires, R.L. Reis, Cork: current technological developments and future perspectives for this natural, Renewable, and Sustainable Material, ACS Sustain. Chem. Eng. 5 (12) (2017) 11130–11146.
[22] S.P. Silva, M.A. Sabino, E.M. Fernandes, V.M. Correlo, L.F. Boesel, R.L. Reis, Cork: properties, capabilities and applications, Int. Mater. Rev. 50 (6) (2005) 345–365.
[23] M. Sahin, E. Ayranci, Electrooxidation of NADH on modified screen-printed electrodes: effects of conducting polymer and Nanomaterials, Electrochim. Acta 166 (2015) 261–270.
[24] W.W.P. Lai, Y.C. Lin, Y.H. Wang, Y.L. Guo, A.Y.C. Lin, Occurrence of emerging contaminants in aquaculture waters: cross-contamination between aquaculture systems and surrounding waters, Water Air Soil Pollut. 229 (8) (2018).
[25] S. Afsa, K. Hamden, P.A.L. Martin, H.B. Mansour, Occurrence of 40 pharmaceutically active compounds in hospital and urban wastewaters and their contribution to Mahdia coastal seawater contamination, Environ Sci Pollut R 27 (2) (2020) 1941–1955.
[26] R. Lulijwa, E.J. Rupia, A.C. Alfaro, Antibiotic use in aquaculture, policies and regulation, health and environmental risks: a review of the top 15 major producers, Rev. Aquac. 12 (2) (2020) 640–663.
[27] I. Campestrini, O.C. de Braga, I.C. Vieira, A. Spinelli, Application of bismuth-film electrode for cathodic electroanalytical determination of sulfadiazine, Electrochim. Acta 55 (17) (2010) 4970–4975.
[28] K.K. Tadi, R.V. Motghare, V. Ganesh, Electrochemical detection of sulfanilamide using pencil graphite electrode based on molecular imprinting technology, Electroanalysis 26 (11) (2014) 2328–2336.
[29] O.C. Braga, I. Campestrini, I.C. Vieira, A. Spinelli, Sulfadiazine determination in pharmaceuticals by electrochemical reduction on a glassy carbon electrode, J. Braz. Chem. Soc. 21 (5) (2010) 813–820.
[30] L. Uzun, A.P.F. Turner, Molecularly-imprinted polymer sensors: realising their potential, Biosens. Bioelectron. 76 (2016) 131–144.
[31] V.K. Gupta, M.L. Yola, N. Ozaltin, N. Atar, Z. Ustundag, L. Uzun, Molecular imprinted polypyrrole modified glassy carbon electrode for the determination of tobramycin, Electrochim. Acta 112 (2013) 37–43.
[32] I.L. Ngo, S. Jeon, C. Byon, Thermal conductivity of transparent and flexible polymers containing fillers: a literature review, Int. J. Heat Mass Transf. 98 (2016) 219–226.
[33] A.C. Fisher, Electrode Dynamics, Oxford University Press, New York, United States, 2009.
[34] D. Martin-Yerga, E.C. Rama, A.C. Garcia, Electrochemical study and determination of electroactive species with screen-printed electrodes, J. Chem. Educ. 93 (7) (2016) 1270–1276.
[35] K.K. Mistry, S.T. Deepthy, C.R. Chaudhuri, H. Saha, Electrochemical characterization of some commercial screen-printed electrodes in different redox substrates, Curr. Sci. 109 (8) (2015) 1427–1436.
[36] A. Bard, L. Faulkner, Electrochemical methods: fundamentals and applications, 1980.
[37] R.H. Wopschall, I. Shain, Effects of adsorption of electroactive species in stationary electrode polarography, Anal. Chem. 39 (13) (1967) 1514–1527.
[38] S.J. Konopka, B. McDuffie, Diffusion coefficients of ferri- and ferrocyanide ions in aqueous media, using twin-electrode thin-layer electrochemistry, Anal. Chem. 42 (14) (1970) 1741–1746.
[39] A.M.O. Brett, C.M.A. Brett, Electrochemistry: Principles, Methods, and Applications, Oxford Science Publications, Oxford University, 1993.
[40] P.T. Kissinger, W.R. Heineman, Cyclic voltammetry, J. Chem. Educ. 60 (9) (1983) 702.
[41] A. Bello, M. Giannetto, G. Mori, R. Seeber, F. Terzi, C. Zanardi, Optimization of the DPV potential waveform for determination of ascorbic acid on PEDOT-modified electrodes, Sensor Actuat B-Chem 121 (2) (2007) 430–435.
[42] A. Menaker, V. Syritski, J. Reut, A. Opik, V. Horvath, R.E. Gyurcsanyi, Electrosynthesized surface-imprinted conducting polymer microrods for selective protein recognition, Adv. Mater. 21 (22) (2009) 2271.